2011 American Control Conference
on O'Farrell Street, San Francisco, CA, USA
June 29 - July 01, 2011

Controller for Reducing Excursions in Tensions, Thicknesses and Looper Positions during Threading of a Hot Metal Strip Rolling Process

John Pittner, *Member, IEEE*, and Marwan A. Simaan, *Fellow, IEEE*

***Abstract*—The highly complex and nonlinear nature of the tandem hot metal strip rolling process presents a difficult control challenge. The control of the threading phase of this process is especially difficult as, in addition to the hostile rolling environment which precludes the location of certain sensors important for control, the model of the process changes rapidly as the head end of the strip is sequenced from stand to stand during threading. To improve the quality of the final product during threading it is necessary to reduce excursions in the strip tension, looper position, as well as strip thickness. This paper extends our previous work to develop an improved controller for this process to include the threading phase. The controller resulting from our previous work in this area is based on the use of an augmented state-dependent Riccati equation technique which has been shown by simulation to be highly successful for control of the threaded tandem mill. In this paper we present a comprehensive model of the threading process plus the results of our initial work to develop a suitable controller which handles the rapid changes in the model during threading. Simulations demonstrate the successful results of this work.**

I. Introduction

THE tandem rolling of hot metal strip in a finishing mill is a significant process in the manufacturing and processing of metals. In the case of steel, almost one-half of the finished product made in the world is originally produced in a hot strip rolling process, which in a great many cases includes a tandem hot strip finishing mill.

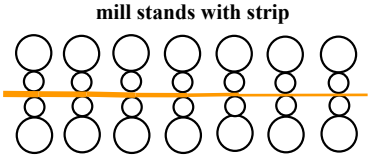

Fig. 1. Typical tandem hot strip finishing mill

Fig. 1 depicts a typical tandem hot strip finishing mill wherein large metal slabs which have been produced in a previous rolling or casting operation are placed in a reheating furnace and heated to temperatures suitable for intermediate processing and subsequent entry into the tandem hot strip finishing mill. In the mill the strip is passed through a set of five to seven pairs of independently driven work rolls, with each work roll supported by a back-up roll of larger diameter. Between each pair of work rolls there is a looper which is a mechanism consisting of an arm and roll driven by hydraulics to keep the strip at a reference tension when the looper is in contact with the strip. Fig. 2 shows a typical schematic for two adjacent mill stands and a looper.

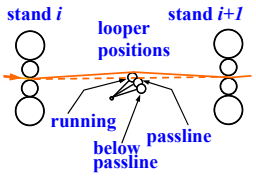

Fig. 2. Looper schematic

The thickness is successively reduced as the strip passes through the individual pairs of work rolls. During threading the head end of the strip is introduced into the upstream stand with the looper below passline. As the strip moves toward the downstream stand the looper is raised such that contact with the strip at passline position is made slightly after the head end of the strip has been threaded into the downstream stand. The looper is then moved to the running position.

During the looper movement it is desired to reduce the excursions in tension to enhance the quality of the final product exiting the mill. Of particular concern is the tension excursion occurring when the looper roll first contacts the strip. In addition, deviations in the strip thickness at the mill area associated with the looper, plus deviations in the tensions, looper positions, and thicknesses in the upstream mill areas (previously threaded), should be reduced during the looper movement.

Generally, conventional looper control applies torque to the looper arm when the strip is in the downstream stand with the looper below passline. When the looper first contacts the strip often there is a high excursion in strip tension. Certain advanced controllers have been proposed, such as those based on model predictive control techniques using linearized models, and simulations have shown some improvements in reducing the tension excursion. However, many of the conventional and the more advanced techniques

Manuscript received September 24, 2010. This work is supported in part by the National Science Foundation under grant 0951843.

J. Pittner is with the University of Pittsburgh, Department of Electrical and Computer Engineering, Pittsburgh, PA 15261 USA (corresponding author; phone: 412-624-1592; fax: 412-624-8003; e-mail: jpittner@engr.pitt.edu).

M. A. Simaan is with the University of Central Florida, Department of Electrical Engineering and Computer Science, Orlando, FL 32816 USA (e-mail: simaan@eecs.ucf.edu).

consider only the tension and looper position during threading without specifically addressing the interactions with the strip thickness or with the already threaded portions of the mill. Thus the issues for a suitable controller must consider both the looper and the already threaded portions of the mill.

The control method presented in this paper considers the looper plus the threaded portions of the mill as a single entity so that interactions between the various mill variables are fully addressed. The techniques which are completely described herein are based on previous work [1], [2] which considers the entire mill as a single entity during the running phase.

In section II a mathematical model for threading is developed, section III presents the controller, simulation results are given in section IV and a conclusion in section V. Unless otherwise noted, the symbols used herein are as listed in Table I.

TABLE I
LISTING OF SYMBOLS

$A(x)$ state-dependent matrix	P specific roll force
$a(x)$ state-dependent vector	$Q(x)$ state weighting matrix
B control matrix	R undeformed work roll radius
$C(x)$ state-dependent output matrix	R_p deformed work roll radius
E Young's modulus	$R(x)$ control weighting matrix
e subscript, estimated value	S roll gap actuator position
F total rolling force	S_0 intercept of mill stretch approximation
f forward slip	T strip temperature (deg C)
$g(x)$ state-dependent vector	t time (seconds)
h strip thickness	U_{Mlpr} looper torque controller ref
i subscript, stand i	U_S roll gap actuator ref
in subscript, stand input	U_V work roll speed actuator ref
J performance index	u control vector
J_{lpr} looper moment of inertia	V_0 work roll peripheral speed
$K(x)$ solution to Riccati equation	V strip speed
k constrained yield stress	W strip width
k_{vis} viscous friction constant	x state vector
L_0 length between c/l of stands	y output vector
L strip length between stands	δ draft = $h_{in} - h_{out}$
M mill modulus	θ looper angle
M_{bnd} looper torque, bending	σ tension stress
M_{fct} looper torque, friction	$\bar{\sigma}$ av tension stress = $(\sigma_{in} + \sigma_{out})/2$
M_{ld} looper torque, total load	τ_d interstand time delay
M_{lmas} looper torque, lpr mass	τ_M time constant, looper torq controller
M_{lpr} torque applied to looper	τ_S time constant, roll gap pos controller
M_{swt} looper torque, strip weight	τ_V time constant, work roll spd controller
M_{ten} looper torque, strip tension	ϕ_n angle at neutral plane
m subscript, measured value	ω looper angular velocity
o or op subscript, operating pt value	A' indicates transpose of matrix A
out subscript, stand output value	$\in C^k$ elements of matrix or vector has continuous partial derivatives thru order k

II. MATHEMATICAL MODEL

A mathematical process model for the running phase has been previously developed. The complete detail of the model and its verification are described in [3], [4]. This model is modified to describe the mill during threading. The salient features of this model and the modifications to it are presented herein for the reader's convenience. A method of active compensation for mill roll eccentricity is assumed to be operable so that any eccentricity components remaining after compensation are taken to be insignificant. For purposes of this investigation Young's modulus, workpiece width, and density are taken to be constant.

A. Model for the Running Phase

During the running phase the operating point of the mill is based on a fully threaded condition at operating speed with a strip tension of 0.01 kN/mm^2 between adjacent stands, and with each looper at an angle of 15 degrees. Table II lists the operating point strip thickness h_{out}, the average strip temperature T at the mill entry and at the exit of each stand, the peripheral speed V_0 of the work rolls, and the undeformed work roll radius R of each stand.

TABLE II
MILL OPERATING POINT

Stand	h_{out} (mm)	T (^{0}C)	V_0 (m/sec)	R (mm)
entry	38.8	1058	----	----
1	21.6	988	1.188	360
2	14.4	973	1.823	336
3	8.6	957	2.957	353
4	6.1	938	4.294	343
5	4.7	922	5.665	388
6	3.9	904	6.946	348
7	3.5	894	7.880	369

The basis for the prediction of the roll force in the roll bite area is Sims' model [5] which we have enhanced by using the comprehensive empirical results of Shida [6] to better estimate the constrained yield stress of the material being rolled. In Sims' model the specific roll force is represented as

$$P = (k Q_p - \bar{\sigma})\sqrt{R_p \delta}\,, \tag{1}$$

where Q_p is a factor developed in Sims' paper which compensates for friction and any inhomogeneities of deformation, and R_p is estimated using the Hitchcock approximation [7]. The exit thickness h_{out} is estimated using the linearized relation for the output thickness as

$$h_{out} = S + S_0 + \frac{F}{M}\,, \tag{2}$$

where the total rolling force $F = PW$, and M represents the elastic stretch of the mill stand under the application of F.

The forward slip f is a measure of the strip speed exiting the roll bite and is defined as the ratio of the relative velocity of the exiting strip to the peripheral speed of the roll,

$$f = \frac{V_{out} - V_0}{V_0}\,. \tag{3}$$

A model that describes the forward slip and is more useful for control development is that presented in Ford, Ellis, and Bland [8] for cold metal rolling, except that for hot rolling the empirical relationship given in Roberts [9] for the coefficient of sticking friction is used in place of the coefficient for sliding friction which is used for cold rolling.

A relationship for strip tension is derived from the relationship for Young's modulus,

$$\frac{d\sigma}{dt} \equiv \dot{\sigma} = \frac{E}{L_0}\left[\frac{dL(\theta(t))}{dt} + V_{in,i+1} - V_{out,i}\right], \ \sigma(0) = \sigma_0 . \quad (4)$$

The position of the hydraulic cylinder that sets the work roll position at the roll bite, and the peripheral speed of the work rolls, are modeled as single first order lags,

$$\frac{dS}{dt} = \frac{U_S}{\tau_S} - \frac{S}{\tau_S}, \qquad S(0) = S_0 , \quad (5)$$

$$\frac{dV}{dt} = \frac{U_V}{\tau_V} - \frac{V}{\tau_V}, \qquad V(0) = V_0 . \quad (6)$$

The interstand time delay is the time taken for an element of strip to move between adjacent stands and is approximated as

$$\tau_{d,i,i+1} = \frac{L}{V_{out,i}}. \quad (7)$$

The looper position angle is determined as

$$\frac{d\theta}{dt} = \omega , \qquad \theta(0) = \theta_0 , \quad (8)$$

where ω is derived from Newton's second law of motion as

$$\frac{d\omega}{dt} = \frac{1}{J_{lpr}}\left[M_{lpr} + M_{fct} + M_{ld}\right], \quad \omega(0) = 0 , \quad (9)$$

with $M_{ld} = M_{ten} + M_{swt} + M_{lmas} + M_{bnd}$. The steady state values of the torques and the value of J_{lpr}, are as given in the Appendix. The torque M_{lpr} is approximated as a first order lag which includes the looper hydraulic cylinder with its controller,

$$\frac{dM_{lpr}}{dt} = \frac{U_{M_{lpr}}}{\tau_M} - \frac{M_{lpr}}{\tau_M}, \quad M_{lpr}(0) = M_{lpr,0} . \quad (10)$$

The friction torque of the looper mechanism is approximated for this investigation as

$$M_{fct} = k_{vis}\,\omega . \quad (11)$$

Detailed calculations for the looper torques, moment of inertia, and $dL(\Theta(t))/dt$ are as given in [4].

The equations of the model representing the nonlinear process dynamics initially are expressed in the form

$$\dot{x} = a(x) + Bu , \quad x(0) = x_0 , \quad (12)$$

$$y = g(x) , \quad (13)$$

where $x \in R^n$ is a vector whose elements represent the individual state variables, $a(x) \in R^n$ is a state-dependent vector, $y \in R^p$ is a vector whose elements represent the individual output variables, $g(x) \in R^p$ is a state-dependent vector, $u \in R^m$ is a vector whose elements represent the individual control variables, and $B \in R^{nxm}$ is a constant matrix. The variables represented by the elements of the state, control, and output vectors are as shown in Table III, where U represents a control reference.

For use in the controller simulation, (12) and (13) are modified to be expressed as

$$\dot{x} = A(x)x + Bu, \ \ x(0) = x_0 , \quad (14)$$

$$y = C(x)x , \quad (15)$$

where $a(x)$ and $g(x)$ are factorized (nonuniquely) into the forms $A(x)x$ and $C(x)x$, where $A(x) \in R^{nxn}$ is a state-dependent matrix, $C(x) \in R^{pxn}$ is a state-dependent matrix, and with x, y, u, and B as previously noted. The elements of the $A(x)$, $C(x)$, and B matrices are as listed in [4].

The variables represented by the elements of the state vector as noted in Table III are directly measured with negligible dynamics, or are similarly derived from measured variables using simple algebraic expressions, so that all the states are available. Variables represented by the elements of the output vector are similarly determined.

TABLE III.
STATE , CONTROL, AND OUTPUT VECTOR VARIABLE ASSIGNMENTS

State Vector		Control Vector	Output Vector	
x_1 (σ_{12})	x_{21} (M_{12})	u_1 (U_{S1})	y_1 (h_{out1})	y_{14} (P_1)
x_2 (σ_{23})	x_{22} (M_{23})	u_2 (U_{S2})	y_2 (h_{out2})	y_{15} (P_2)
x_3 (σ_{34})	x_{23} (M_{34})	u_3 (U_{S3})	y_3 (h_{out3})	y_{16} (P_3)
x_4 (σ_{45})	x_{24} (M_{45})	u_4 (U_{S4})	y_4 (h_{out4})	y_{17} (P_4)
x_5 (σ_{56})	x_{25} (M_{56})	u_5 (U_{S5})	y_5 (h_{out5})	y_{18} (P_5)
x_6 (σ_{67})	x_{26} (M_{67})	u_6 (U_{S6})	y_6 (h_{out6})	y_{19} (P_6)
x_7 (S_1)	x_{27} (θ_{12})	u_7 (U_{S7})	y_7 (h_{out7})	y_{20} (P_7)
x_8 (S_2)	x_{28} (θ_{23})	u_8 (U_{V1})	y_8 (σ_{12})	y_{21} (θ_{12})
x_9 (S_3)	x_{29} (θ_{34})	u_9 (U_{V2})	y_9 (σ_{23})	y_{22} (θ_{23})
x_{10} (S_4)	x_{30} (θ_{45})	u_{10} (U_{V3})	y_{10} (σ_{34})	y_{23} (θ_{34})
x_{11} (S_5)	x_{31} (θ_{56})	u_{11} (U_{V4})	y_{11} (σ_{45})	y_{24} (θ_{45})
x_{12} (S_6)	x_{32} (θ_{67})	u_{12} (U_{V5})	y_{12} (σ_{56})	y_{25} (θ_{56})
x_{13} (S_7)	x_{33} (ω_{12})	u_{13} (U_{V6})	y_{13} (σ_{67})	y_{26} (θ_{67})
x_{14} (V_1)	x_{34} (ω_{23})	u_{14} (U_{V7})		
x_{15} (V_2)	x_{35} (ω_{34})	u_{15} (U_{Mlpr12})		
x_{16} (V_3)	x_{36} (ω_{45})	u_{16} (U_{Mlpr23})		
x_{17} (V_4)	x_{37} (ω_{56})	u_{17} (U_{Mlpr34})		
x_{18} (V_5)	x_{38} (ω_{67})	u_{18} (U_{Mlpr45})		
x_{19} (V_6)		u_{19} (U_{Mlpr56})		
x_{20} (V_7)		u_{20} (U_{Mlpr67})		

B. Modifications for Threading

For each looper two cases are identified that require modifications to the model for the running phase. These are: (1) strip in the upstream stand, not yet in the downstream stand, and with the looper below passline; and (2) strip in the upstream and downstream stands, with the looper remaining below passline. The modifications to the model for running for each of these cases are as follows.

For case (1) the interstand tension is zero and the looper is decoupled from the remainder of the model. In this case $\dot{\sigma}$ and $\sigma(0)$ in (4), and $M_{ten}, M_{swt}, M_{bnd}$ in M_{ld} of (9) are zero, with the state, control, and output vectors (Table III) adjusted accordingly for independent control of the looper. For case (2) the interstand tension is no longer zero, with the looper remaining uncoupled from the rest of the model. In this case $\dot{\sigma}$ is as given in (4), and $M_{ten}, M_{swt}, M_{bnd}$ remain at zero, with the state, control, and output vectors readjusted accordingly for control of strip tension by the SDRE-based controller, with the independent control of the looper

remaining. The looper is considered to be coupled to the rest of the model when it is in contact with the strip. In this case the model is as described above for running.

III. CONTROLLER

A. The State-dependent Riccati Equation Technique

A brief overview of the state-dependent Riccati equation (SDRE) technique follows. This technique is becoming recognized as a desirable and useful nonlinear method for the control of many nonlinear applications due to its simplicity and its capability for allowing the use of physical intuition in the design process. More detailed treatments of the SDRE method are found in [10]-[12].

The SDRE technique is much like the LQR method except that the control and state weighting matrices and the coefficient matrices in the state and output equations are state-dependent. This technique is developed by expressing the nonlinear plant dynamics in the form as noted previously in (14) and (15). The optimal control problem then is defined in terms of minimizing the performance index

$$J = \frac{1}{2}\int_0^\infty (x'Q(x)x + u'R(x)u)dt \tag{16}$$

with respect to the control vector u, subject to the constraint (14), where $Q(x) \geq 0$, $R(x) > 0$, $Q(x)$ and $R(x) \in C^k$ for $k \geq 1$. Equation (16) essentially implies finding a control law which regulates the system to the origin. The state-dependent algebraic Riccati equation

$$A'(x)K(x) + K(x)A(x) - K(x)BR^{-1}(x)B'K(x) + Q(x) = 0 \tag{17}$$

is solved pointwise for $K(x)$, which results in the control law

$$u = -R^{-1}(x)B'K(x)x\,. \tag{18}$$

The method requires that the pair $(A(x),B)$ be pointwise stabilizable (in a linear sense) for all x in the control space in order to ensure a solution to (17) at each point. While local asymptotic stability is assured under some fairly mild conditions [11], in general asymptotic stability over the entire control space must be confirmed by simulation.

B. Application to the Control of Threading of Tandem Hot Strip Rolling

It is important to reduce excursions in the interstand tensions, thicknesses, and looper positions of the upstream mill stands, as well as in the stand presently being threaded. This is necessary for improvement in the quality of the final product and to assure the stability of rolling. Accordingly the controller is configured to control the looper and the upstream stands as a single entity rather than controlling only the looper position and tension. Based on previous work with the mill entirely threaded, it is expected that the nonlinear MIMO nature of the SDRE technique can provide an effective means of inherently handling the interactions between various variables during threading. As also shown in previous work, the controller can be effective in reducing excursions due to perturbations, such as those resulting from downstream threading actions as the head end of the strip sequences through the mill. The SDRE technique is augmented by outer loop SISO trimming functions (trims) which reduce slight offsets in the looper positions, and provide zero error in the measured tensions and estimated strip thicknesses. The thickness trims are effective in reducing the effects of the interstand time delays on the estimated thickness as they provide a nearly immediate correction to excursions in the estimated thicknesses, while the time delays have little effect on the tension since the tension propagates through the strip as the speed of sound. Moreover, the closed loop control actions of the trims contribute toward reducing the effects of uncertainties as many of these effects occur inside the control loops of the trims.

During threading a major uncertainty is the estimation of the strip tension during the short time that the strip is in both the upstream and downstream stands and with the looper below passline, so that an estimated tension signal based on measured variables associated with the looper is unavailable. With the looper in contact with the strip so that the measured variables required to estimate the tension are available, the uncertainty is taken to be as in the case of running operation.

During threading, prior to when the looper is in contact with the strip, the looper is controlled separately by an independent controller which controls its position as it moves toward the strip. A separate torque reference is provided by the independent controller to the torque controller (10) when the looper is not contacting the strip. After the strip enters the upstream stand the motion is initiated and controlled so that contact with the strip is made just after the strip is in the downstream stand. The position is controlled so that the speed of the looper is reduced as it approaches the strip to reduce excursions in tension during initial contact with the strip. The independent controller is disabled after contact is established. The control of the looper then is switched to that for running operation using the SDRE-based controller, and the looper is raised to running position by moving the operating point of the controller to the operating point for running. During the time that the independent controller is effective, the appropriate elements of the weighting matrices of the SDRE controller are set to zero to prevent the looper position, torque, and speed from influencing the SDRE control of the remainder of the mill that has already been threaded, and the control of the tension and thickness by the SDRE after the strip has entered the downstream stand. During the time that the looper is being raised after contacting the strip and while it is at run position, excursions in tension and thickness are reduced as these variables are controlled by the SDRE-based system. As the strip is threaded through the mill, the control concept, which considers both the looper and the threaded upstream stands is the essentially the same for each looper.

C. Structure of the Controller

Fig. 3 depicts the controller. The SDRE-based system is essentially that as described in [13] for the mill in running operation, except with appropriate modifications for threading. For background and as an aid to the reader a brief description of this system when in the running phase follows, with modification as shown for the threading phase. The effects of disturbances and uncertainties are modeled separately and depicted as shown for simplicity of presentation. The vectors x, u, and y at the operating point are represented as x_{op}, u_{op}, and y_{op}. A coordinate change is performed by the introduction of the vector $z=x-x_{op}$ which shifts the operating point to the origin. The performance index (16) then is modified to be

$$J = \frac{1}{2}\int_0^\infty (z'Qz + (u-u_{op})'R(u-u_{op}))\,dt\,, \qquad (19)$$

where for simplicity Q and R are taken for this initial effort as diagonal matrices with adjustable constant elements. Each element of the state vector x is obtained from measured variables, certain elements of the output vector y are represented by the vector y_m, y_e is a vector whose elements are the tension and thickness feedbacks used in the trims, and φ_y is an algorithm which generates y_e by using simple algebraic relationships involving its inputs and having no dynamics. The K_P and K_I blocks are diagonal matrices whose elements are the gains for the PI trims for the tensions and thicknesses. The switching function selects the looper torque reference to be from the controller for normal running or from the independent controller (not shown) when the looper is not in contact with the strip.

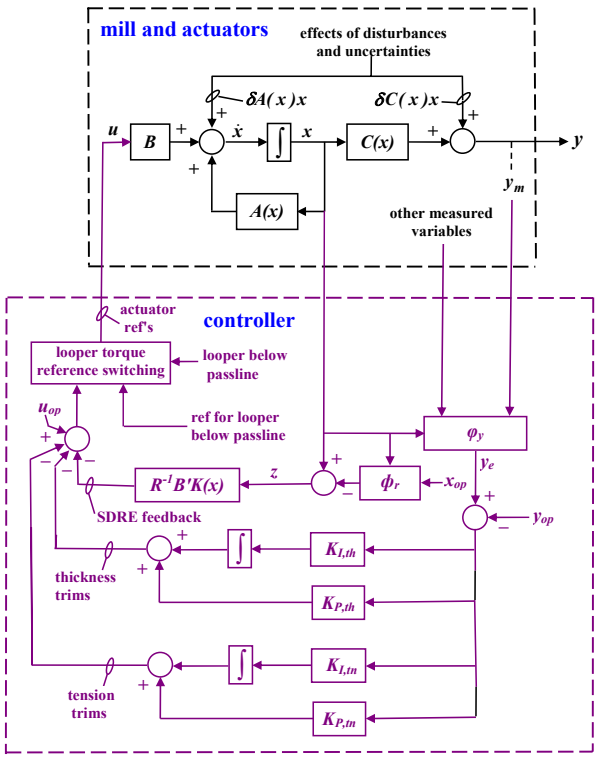

Fig. 3. Structure of the controller

For operation with the looper in contact with the strip, the algorithm ϕ_r represents the looper operating point trims which are implemented as shown in Fig. 4 where $x_{op,i}$ $(i=27,\ldots,32)$ is an element of the vector x_{op} that represents the operating point for the looper between stands $i,i+1$, $l_{i,i+1,ref}$ is the looper reference for stands $i,i+1$, x_i is the element of the state vector which represents the measured looper position for stands $i,i+1$, and $K_{i,i+1}$ is a gain term for stands $i,i+1$. A direct feed-through is provided for the remaining elements of $x_{op,i}$.

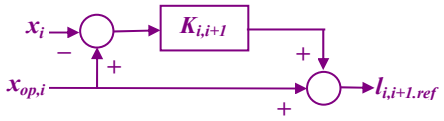

Fig. 4 Operating point trim for looper angle

The pointwise solving of (17) sufficiently fast (7 ms) to properly control the process is assured by use of the matrix sign function technique [14].

IV. Simulation

Simulations (closed-loop) were performed using MATLAB/Simulink with the controller (Fig. 3) coupled to the model and using the mill and looper properties as given in the Appendix. The mill exit speed is taken as 7.15 m/sec with an exit speed at stand 1 of 1.21 m/sec. The time for the head end of the strip to move from stand 1 to stand 2 is about 4.5 sec. The operating point of the running condition is based on the data of Table II. The settings of the elements of the diagonal Q and R matrices and the gain settings of the trims were made intuitively and confirmed by simulation.

For this initial evaluation, simulations were performed for threading the mill between stands 1 and 2. The looper position was initially assumed to be at zero (below passline), with a passline position of 0.0506 rad (2.9 degrees) and a run position of 0.2618 rad (15 degrees). The head end of the strip is assumed to be roughly tracked from the exit of stand 1, so that the looper movement toward passline is initiated such that the looper contacts the strip as the head end is threaded into and slightly past stand 2.

An uncertainty of +10% was assumed for the tension for the short time that the looper is not in contact with the strip and the strip is in both the upstream and downstream stands, and –1% after contact is made and useful measurements are available for estimating the tension. The separate controller was simulated as a position controller which provides a reference to an inner torque control loop that controls the looper hydraulic cylinder. For the purposes of this initial evaluation, it was assumed that other uncertainties and disturbances would be addressed as part of ongoing work.

The results are shown in Fig. 5 and Fig. 6. As shown in these figures, the excursion in tension is very small with respect to the uncertainty in the tension estimate, and the total excursion in tension is about 3% during the overall movement from below passline to run position. Moreover,

the deviation in strip thickness was held to less than 0.05 % during the looper movement.

This compares well with typical deviations in tension on the order of 50-200% for general conventional control methods and about 25-50% for certain more advanced control schemes. However, much more remains to be done as part of ongoing work to fully evaluate the control performance as the strip is threaded throughout the entire mill, including an expanded evaluation of the effect of perturbations during threading on upstream areas in the mill that are already threaded, and the consideration of the effects of various uncertainties and disturbances.

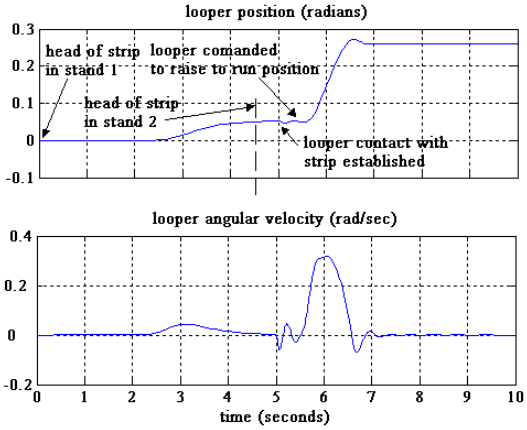

Fig. 5. Looper position and angular velocity

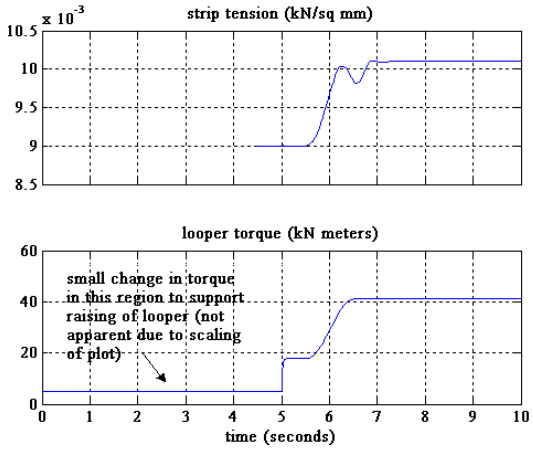

Fig. 6. Strip tension and looper torque

V. Conclusion

The results of this initial effort show that the new controller offers a strong potential for reducing excursions in the strip tensions and thicknesses, and in the looper positions during threading. While a good deal more remains to be done, based on this initial work it is considered that this approach leads to a significant improvement in the quality of the final output of the tandem hot metal rolling process and therefore is worthy of ongoing investigation.

Appendix

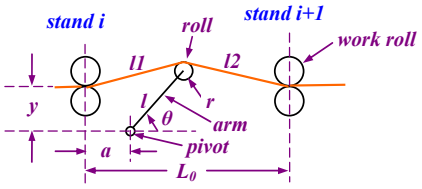

Fig. 7 Looper detail

Looper Characteristics

Dimensions: L_0 = 5.478 m, y = 0.191 m, a = 1.943 m, r (radius) = 0.152 m, l = 0.762 m. Max angle: 40 deg. Pass line angle: 2.9 deg. Mass of looper arm: 300 kg. Mass of looper roll: 500 kg. Viscous friction constant: k_{vis} = –2.0 kNm/rad/sec. Moment of inertia: J_{lpr} = 0.3542 (in kgm^2/1000). At the steady-state operating point: θ = 15 deg, ω = 0 rad/sec, $l1$ = 2.684 m, $l2$ = 2.806 m, M_{ten} = –4.289 kNm, M_{swt} = –1.515 kNm, M_{lmas} = –4.693 kNm, M_{bnd} = –0.132 kNm, M_{fct} = 0 kNm, M_{ld} = –10.629 kNm, and M_{lpr} = 10.629 kNm.

References

1. J. Pittner and M. A. Simaan, *Tandem Cold Metal Rolling Mill Control*, Chapter 5, Springer-Verlag, London, 2011.
2. J. Pittner and M. A. Simaan, "Quality improvement of tandem hot metal strip rolling using an augmented state-depedent Riccati equation technique," *Proceedings of the 2010 Conference on Decision and Control,* Atlanta, GA, pp. 5180-5185.
3. J. Pittner and M. A. Simaan, "An initial model for control of a tandem hot metal strip rolling process," *IEEE Transactions on Industry Applications*, **46**(1), pp. 46-53, 2010.
4. J. Pittner and M. A. Simaan, "A useful control model for tandem hot metal strip rolling," *IEEE Transactions on Industry Applications*, **46**(6), pp. 2251-2258, 2010.
5. R. B. Sims, "The calculation of roll force and torque in hot rolling mills," *Proceedings of the Institution of Mechanical Engineers*, Vol. 168, pp. 191-200, UK, 1954.
6. M. Pietrzyk and J. G. Lenard, , *Thermal-mechanical modeling of the flat rolling process*, pp. 12-13, Springer-Verlag, Berlin, 1991.
7. Lenard, J. G., Pietrzyk, M., and Cser, L., *Mathematical and Physical Simulation of Hot Rolled Products*, p. 91, Elsevier, Amsterdam, 1999.
8. H. Ford, E. F. Ellis, and D. R. Bland., "*Cold rolling with strip tension, part I-A new approximate method of calculation and comparison with other methods*," Journal of the Iron and Steel Institute, Vol. 168, pp.57-72, UK, May, 1951.
9. W. L. Roberts, *Hot Rolling of Steel*, page 782, Marcel Dekker, New York, 1983.
10. T. Cimen, "State-dependent Riccati equation (SDRE) control: A survey," in *Plenary Papers, Milestone Reports, and Selected Survey Papers*, edited by Myung Jin Chung and Pradeep Misra, *17th IFAC World Congress*, Seoul, Korea, 2008.
11. J. R. Clautier, N. D'Souza, and C. P. Mracek, "Nonlinear regulation and nonlinear H^{∞} control via the state-dependent Riccati equation technique: Part 1, theory," *Proceedings of the International Conference on Nonlinear Problems in Aviation and Aerospace*, Embry Riddle University, pp. 117-131, 1996.
12. J. R. Cloutier and D. T. Stansbery, "The capabilities and art of state-dependent Riccati equation-based design," *Proceedings of the American Control Conference*, Anchorage, Alaska, May 2002.
13. J. Pittner and M. A. Simaan, "Controller for improving the quality of the tandem rolling of hot metal strip," in *Proceedings of the 2010 American Control Conference*, Baltimore, MD, pp 6095-6100.
14. C. S. Kenney and A. J. Laub, "The matrix sign function," *IEEE Transactions on Automatic Control*, Vol. 40, No. 8, pp.1330-1348, 1995.